[11] Bevilaqua, P. M., and Lykoudis, P. S., "Turbulence Memory in Self-Preserving Wakes," *Journal of Fluid Mechanics*, Vol. 89, July 1978, pp. 589–606.
[12] Carmody, T., "Establishment of the Wake Behind a Disk," *Journal of Basic Engineering*, Vol. 87, Dec. 1964, pp. 869–882.

F. W. Chambers
Associate Editor

Hemisphere-Cylinder in Dynamic Pitch-Up Motions

O. K. Rediniotis*
Texas A&M University, College Station, Texas 77843-3141
N. T. Hoang†
AURORA Flight Sciences Corporation, Manassas, Virginia 20110
and
D. P. Telionis‡
Virginia Polytechnic Institute and State University, Blacksburg, Virginia 24061

I. Introduction

THE flows over various axisymmetric bodies such as ogive-cylinders, hemisphere-cylinders, and prolate spheroids have been studied numerically and experimentally by many investigators. An extensive literature review can be found in Ref. 1. An interesting feature of the flow over axisymmetric bodies at large incidence is the asymmetry of the mean vortical patterns of the wake. This phenomenon has been well documented for pointed bodies such as conical and ogive-cylinder bodies.[2,3] Flows over such bodies are sensitive to many parameters, such as irregularities at the nose, surface roughness, body length, slenderness of the nose, angle of attack, freestream turbulence, and Reynolds number. Moskovitz et al.[2] investigated the effects of geometric perturbations on the asymmetric flow past an ogive/cone cylinder. Roos and Kegelman[3] studied asymmetric flows at angles of attack up to 60 deg over three generic forebodies, namely ogive, elliptical, and chined bodies. Blunt-nosed models are less prone to asymmetry. Forced asymmetric wake patterns over blunt-nosed cylinders have been experimentally documented by Hoang and Telionis.[4]

In all of these efforts, steady-state flowfields with the models at fixed angles of attack were investigated. Very little has been published on the flowfield development over dynamically maneuvering bodies. A numerical investigation was carried out by Ying et al.[5] on dynamic motions of slender bodies. However, the work was not substantiated by experimental comparison. Stanek and Visbal[6] have also calculated the flow over a pitching slender body. The reduced pitch rates employed there were much larger than the ones considered here. Experimental efforts on pitching slender bodies have been confined to flow visualizations or force measurements.[7–9]

The purpose of the present investigation is to extend our understanding of the development of the leeward vortices over a hemisphere-cylinder and, in particular, asymmetric leeward vortices under unsteady conditions. This was accomplished by placing a hemisphere-cylinder model in a steady flowfield and mechanically pitching it about its nose. The unsteady development of the wake is studied. To induce vortex asymmetry a disturbance is introduced on the nose of the hemisphere-cylinder.

Received 16 June 1997; revision received 20 March 1998; accepted for publication 8 March 1999.

*Assistant Professor, Aerospace Engineering Department.
†Research Scientist.
‡Frank J. Maher Professor, Engineering Mechanics Department.

II. Facilities, Instrumentation, and Experimental Conditions

The work was conducted in the Engineering Science and Mechanics (ESM) water tunnel through laser Doppler velocimetry (LDV). The water tunnel has a 25.4 × 30.5 cm test section and can achieve speeds up to 3 m/s at turbulence levels ranging from 0.6 to 1.5%. Three-component LDV was employed in the water tunnel. The system employed is a Thermal Systems, Inc. (TSI) LDV system operating in backscatter mode with a 35 mW helium–neon laser. An assembly of mirrors and traversing mechanisms operated by stepping motors facilitates displacement of the measuring volume. Measuring grids normal to the oncoming stream can thus be automatically traversed. The measuring volume can be positioned on a grid point with an accuracy of 0.1 mm through the use of two linear variable differential transformers (LVDTs) that are integrated in a position feedback loop. The entire data-acquisition operation is controlled by serially communicating laboratory computers that are programmed to operate the pitching mechanism and the traversing systems, collect the information on the instantaneous angle of attack, perform the LDV data acquisition, reduce the data, and transfer the data to a mainframe IBM 3090 for postprocessing and presentation. Detailed information on the LDV instrumentation and data-acquisition scheme can be found in Ref. 10. The hemisphere-cylinder model tested was provided by the Fluid Dynamics Branch of NASA Langley Research Center. The model was machined out of aluminum, with an overall length of $L = 14.73$ cm and a diameter of $D = 2.95$ cm.

Experiments were conducted with a fixed as well as with a dynamically pitching model. The dynamic motion chosen was a pitch-up about the nose, followed by a slow return to the initial angle of attack. Data were obtained at 100 time instants during the pitch-up and were ensemble averaged. To decide on the number of realizations per ensemble average, we took measurements over 50 realizations at representative wake locations. For each location, ensemble averages

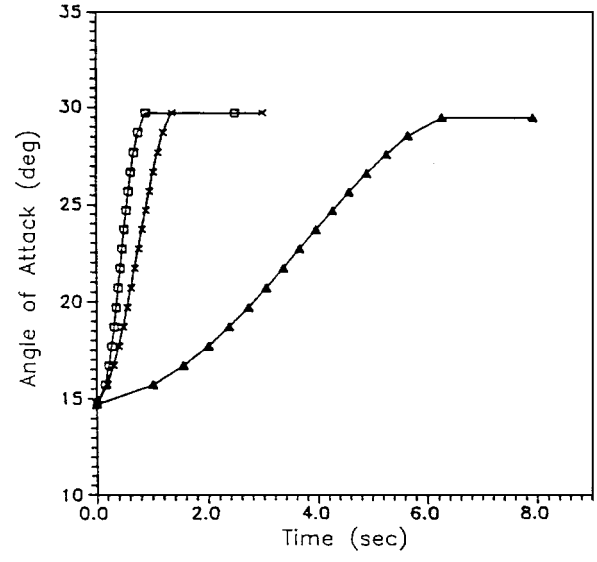

Fig. 1 Time schedules for the pitch-up motions: ▲, $k_2 = 1.4 \times 10^{-3}$; ×, $k_3 = 6 \times 10^{-3}$; and □, $k_4 = 1 \times 10^{-2}$.

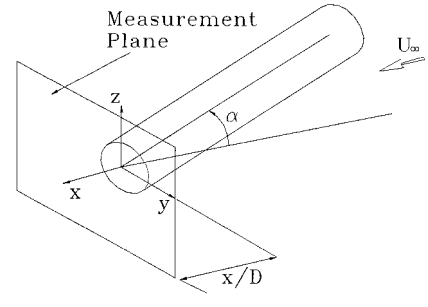

Fig. 2 Model and coordinate system.

were then calculated by considering 5, 7, 10, 15, 25, and 50 of these realizations, respectively. For a number of realizations of seven and higher, the results varied by less than 3%. This was considered an acceptable error. The data presented in this Note were averaged over seven realizations. Notice that the estimated velocity measurement uncertainty for the LDV system was 2.5%.

A trigger to the data-acquisition hardware was provided from the pitching mechanism. In addition, an encoder recorded the instantaneous angle of attack at each of the sampling time instants. The model was pitched up from $\alpha = 15$ to 30 deg. The dimensionless pitch rate is defined as $k = \omega D/2U_\infty$, where D and U_∞ are the model diameter and the freestream velocity, respectively, and ω is the average angular velocity of the pitch-up motion. The dimensionless pitch rates tested were $k_1 = 0.0$ (steady state), $k_2 = 1.4 \times 10^{-3}$, $k_3 = 6 \times 10^{-3}$, and $k_4 = 1 \times 10^{-2}$. Figure 1 presents the pitch-up schedules. It was attempted to generate ramplike pitch-up motions. However, some acceleration and deceleration effects were present at the beginning and the end of the motions. The Reynolds number,

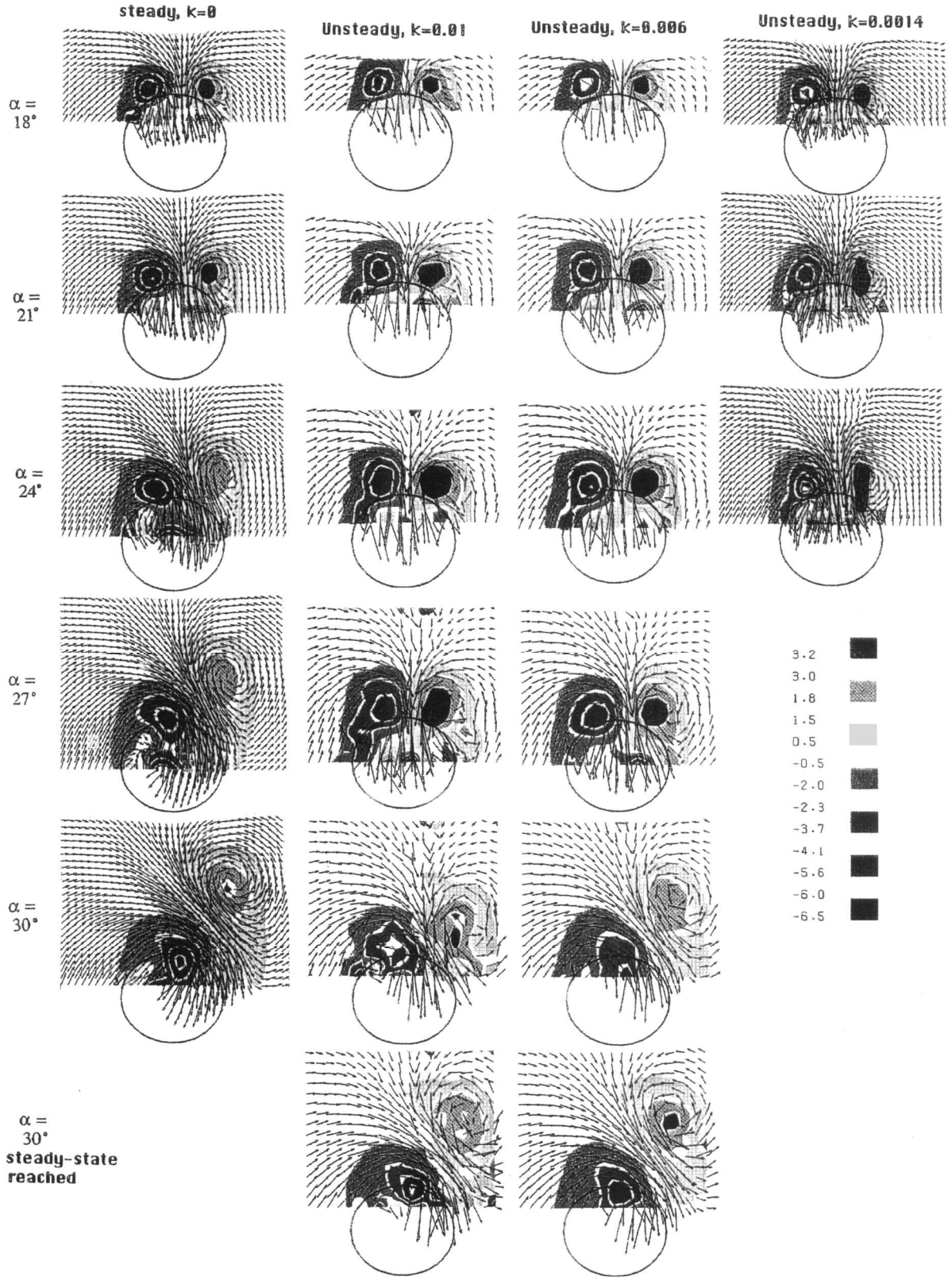

Fig. 3 Axial vorticity contours and crossflow velocity vectors along the measurement plane.

based on freestream velocity and cylinder diameter, was around 1.2×10^4.

Because blunt-nosed cylinders do not develop wake asymmetries as easily as ogive-cylinders, the asymmetry was induced by introducing a disturbance in the form of a hemispherical bump of diameter d, with $d/D = 0.15$, positioned near the nose of the model. The effect of the disturbance position on the flow over blunt-nosed geometries (nose fineness ratio of 0.5) has been carefully explored.[11] In the work presented here, the disturbance was positioned at an azimuthal angle of 120 deg measured from the windward side of the model and at $x'/D = 0.122$, with x' measured along the axis of the model, from the model nose tip. All of the results presented here were obtained along a plane normal to the freestream, downstream of the model back end. The tunnel-fixed coordinate system is shown in Fig. 2, with its origin at the center of the model base when the model is at its initial position, i.e. $\alpha = 15$ deg. In this coordinate system, the position of the measurement plane was $x/D = 0.5$.

III. Results and Discussion

In Fig. 3 we present crossflow velocity distributions, i.e., velocity components in the measurement plane. On the basis of these data, the nondimensional axial component of the vorticity

$$\Omega_x = \frac{D}{U_\infty}\left[\frac{\partial v}{\partial z} - \frac{\partial w}{\partial y}\right] \tag{1}$$

was calculated and presented in terms of color contours. In Eq. (1), v and w are the velocity components along the axes y and z, respectively. For the motion with $k_2 = 1.4 \times 10^{-3}$, the accuracy of the data acquired above $\alpha = 24$ deg was compromised because of difficulties with the experimental setup, and therefore these data are not presented here. The uncertainty in the evaluation of the vorticity was calculated from the uncertainties in the measurement of the velocity and in the positioning of the measurement volume, by using a constant-odds combination.[12] The estimated uncertainty was 4%.

Physical insight into the important flow timescales, as compared with the timescales dictated by the reduced frequencies tested, can be gained by recalling two-dimensional results. If one were to neglect the influence of the model ends, then the flow along a crossflow plane, i.e., a plane normal to the axis of the model, would resemble the flow over a circular-cylinder started from rest. It is well established that unsteady separation develops at a dimensionless time $\tau = tU_\infty/D$ of approximately 1, but a pair of vortices requires about 10 dimensionless time units before growing to its regular size. The time spans of the motions depicted in Fig. 1 based on the maximum crossflow velocity are about 50, 10 and 6 dimensionless time units for $k_2 = 1.4 \times 10^{-3}$, $k_3 = 6 \times 10^{-3}$, and $k_4 = 1 \times 10^{-2}$, respectively. Therefore the motion with $k_2 = 1.4 \times 10^{-3}$ could be considered practically quasi steady, whereas this is not the case for the other two motions. As shown in Fig. 3, in steady state ($k = 0.0$), wake asymmetries caused by the flow disturbance introduced at the nose are first manifested at $\alpha = 24$ deg. In the unsteady cases with $k_3 = 6 \times 10^{-3}$ and $k_4 = 1 \times 10^{-2}$, the vortical flows are initially symmetric. At low angles of attack, there seems to be little deviation between the steady- and the corresponding unsteady-flow patterns. However, in the unsteady cases, after $\alpha = 24$ deg the flow continues developing in a symmetric fashion. The evolution toward asymmetry is now delayed. These results are in qualitative agreement with those of Montividas et al.,[9] who also observed via flow visualization a delay in the development of the vortex asymmetry. However, for the unsteady case with $k_2 = 1.4 \times 10^{-3}$, signs of vortex asymmetry are already exhibited, as in the steady-state case, at $\alpha = 24$ deg.

IV. Conclusions

In the work presented here, LDV was employed to study the dynamic evolution of the wake of the hemisphere-cylinder as a representative of blunt-nosed axisymmetric bodies at incidence. Contrary to pointed axisymmetric bodies, which can sustain highly asymmetric wakes, no such asymmetries exist in the wake of blunt-nosed axisymmetric bodies such as the hemisphere-cylinder. In the case considered here, a disturbance introduced in the nose region results in significant departures from symmetry. This phenomenon was exploited to induce asymmetric wakes and study their dynamic evolution during a model pitch-up maneuver. Velocity data were obtained over a fixed model at a range of angles of attack, as well as over a model pitching dynamically from $\alpha = 15$ to 30 deg, at three nondimensional pitch-up rates. The effect of nondimensional pitching rate on the wake development was documented. The data presented here indicate that vortex wake asymmetries are delayed significantly if the model is pitched up dynamically at nondimensional rates higher than roughly the rate corresponding to a motion period equal to the time required for the leeward vortices to develop downstream of a two-dimensional circular cylinder in flow starting from rest.

Acknowledgment

This work was supported by NASA Langley Research Center under Grant NAS1-18471.

References

[1]Hoang, N. T., Rediniotis, O. K., and Telionis, D. P., "Separation over Axisymmetric Bodies at Large Angles of Attack," AIAA Paper 91-0377, Jan. 1991.

[2]Moskovitz, C. A., Hall, R. M., and DeJarnette, F. R., "Effects of Nose Bluntness, Roughness and Surface Perturbations on the Asymmetric Flow Past Slender Bodies at Large Angle of Attack," AIAA Paper 89-2236, July 1989.

[3]Roos, F. W., and Kegelman, J. T., "Aerodynamic Characteristics of Three Generic Forebodies at High Angles of Attack," AIAA Paper 91-0275, Jan. 1991.

[4]Hoang, N. T., and Telionis, D. P., "The Dynamic Character of the Wake of an Axisymmetric Body at an Angle of Attack," AIAA Paper 91-3268, Sept. 1991.

[5]Ying, S. X., Steger, J. L., Schiff, L. B., and Baganoff, D., "Numerical Simulation of Unsteady, Viscous, High-Angle-of-Attack Flows Using a Partially Flux-Split Algorithm," AIAA Paper 86-2179, June 1986.

[6]Stanek, M. J., and Visbal, M. R., "Investigation of Vortex Development on a Pitching Slender Body of Revolution," AIAA Paper 91-3273, Sept. 1991.

[7]Smith, L. H., and Nunn, R. H., "Aerodynamic Characteristics of an Axisymmetric Body Undergoing a Uniform Pitching Motion," AIAA Paper 75-0638, June 1975.

[8]Gad-el Hak, M., and Ho, C. M., "Unsteady Flow Around an Ogive Cylinder," *Journal of Aircraft*, Vol. 23, No. 6, 1986, pp. 520–528.

[9]Montividas, R. E., Reisenthel, P., and Nagiv, H. N., "The Scaling and Control of Vortex Geometry Behind Pitching Cylinders," AIAA Paper 89-1003, May 1989.

[10]Hoang, N. T., Rediniotis, O. K., and Telionis, D. P., "The Temporal Evolution of a Pair of Streamwise Vortices," *Experiments in Fluids*, Vol. 19, Nov. 1995, pp. 241–249.

[11]Hoang, N. T., Rediniotis, O. K., and Telionis, D. P., "Symmetric and Asymmetric Separation Patterns over a Hemisphere Cylinder at Low Reynolds Numbers and High Incidences," *Journal of Fluids and Structures*, Vol. 11, Oct. 1997, pp. 793–817.

[12]Moffat, R. J., "Contributions to the Theory of Single-Sample Uncertainty Analysis," *Journal of Fluids Engineering*, Vol. 104, June 1982, pp. 250–260.

A. Plotkin
Associate Editor